Supporting Information for

Insights into the effects of pulsed CO_2 electrolysis in a zero-gap electrolyzer

Xiao Kun Lu[1], Weiyan Ni[2, 3], Adrien E. Deberghes[1], Linsey C. Seitz[1, *]

[1]Department of Chemical and Biological Engineering, Northwestern University, Evanston, IL 60208, USA

[2]Department of Chemistry, Northwestern University, Evanston, IL 60208, USA

[3]Department of Electrical and Computer Engineering, Northwestern University, Evanston, IL 60208, USA

Corresponding Author: Linsey C. Seitz (linsey.seitz@northwestern.edu)

Table of Contents

S1. Experimental Methods

Chemicals

All deionized (DI) water used is Millipore quality (18.2 MΩ·cm at 25°C) unless otherwise specified. $KHCO_3$ (ACS, 99.3%) was purchased from Sigma. 2-propanol (ACS) and KOH (ACS) were purchased from Fisher.

Synthesis of CuO

CuO was synthesized based on a previously reported method.[1] Briefly, 100 mg of $CuSO_4$ was dissolved in 4 mL DI water in a round bottom flask while stirred. Then, 2.5 mL of 1 M KOH was added dropwise into the $CuSO_4$ (reagent, Fisher) to solution to form $Cu(OH)_2$ precipitates. After 15 mins stirring, 1 mL ammonium hydroxide (ACS, Honeywell) was added to the solution. The solution was then transferred to a Teflon-lined autoclave (Parr) to be heated at 80°C for 12 h with ramp rate of 1.5°C/min. The resulting solid product was collected by centrifuging at 8500 rpm and washing three times with DI water and once with ethanol.

Electrode Preparation

Catalyst inks for performance tests were prepared from 10 mg Cu nanoparticles (NP) (40-60 nm, Sigma), 1 mL 2-propanol, and a binder solution. Nafion-containing samples used 50 μL Nafion D520 solution (5 wt% Nafion, Ion Power); Sustainion-containing samples used 50 μL Sustainion solution (prepared from Sustainion XA-9, 5 wt% in ethanol, Dioxide Materials), and fluoroethylene propylene (FEP) samples contained 10 μL of FEP dispersion (FEPD 121, Fuel Cell Store). Inks were sonicated for 1 h before use. Cathode gas diffusion electrodes (GDEs) were prepared by spray coating ink mixture onto a 3 x 3 cm^2 carbon gas diffusion layer (Sigracet 39BB, Fuel Cell Store) using an automatic ultrasonic spray coater (60kHz nozzle, Microspray), resulting in 1 mg/cm^2 Cu loading.

Anodes were prepared via a dip coating method where 80 mg of $IrCl_3 \cdot xH_2O$ (reagent grade, Sigma) was dissolved in 9 mL 2-propanol and 1 mL concentrated H_2SO_4 (Sigma). Platinized Ti felt (Fuel cell Store) of 30 cm^2 was dipped in the $IrCl_3$ solution, then dried at 100 °C for 5 min, and calcined in air for 15 min. This process was repeated until all the solution was used up.

Hydrogen evolution reaction (HER) cathodes were prepared by spray coating 1 mg/cm^2 of Pt/C (20 wt%, Alfa Aesar) onto a carbon-based GDL with no microporous layer (Toray TGP-H-60, Fuel Cell Store).

Electrodes for *in situ* Raman spectroscopy were prepared by spray coating an ink of 10 mg CuO, 1 mL 2-propanol, and 50 μL 5 wt% Sustainion XA-9 onto a carbon gas diffusion layer (Toray TGP-H-120 with MPL, Fuel Cell Store).

Membrane Preparation

Sustainion 37-50 membrane (Dioxide Materials) was removed from packaging, cut into 5 x 5 cm^2 pieces, and soaked in 1 M KOH solution for 24 h. The membranes were delaminated from the plastic support after 24 h and stored in fresh 1 M KOH solution before use.

Electrochemical Testing

Electrochemical experiments were performed in a membrane electrode assembly (MEA) with titanium flow plates (5 cm^2 geometric active area, Dioxide materials) and PTFE gaskets. A piece of Sustainion membrane was sandwiched between a Cu-GDE cathode and an IrO_x/Ti anode. The torque for tightening the flow fields was set to 5.6 Nm by a torque wrench.

During electrolysis, humidified CO_2 was fed at 50 s.c.c.m. controlled by a mass flow controller (MKS Instruments) and 0.1 M $KHCO_3$ was circulated at 5 mL/min through the anodic compartment by a peristaltic pump (BT100L, Golander). Electrochemical data was collected with a potentiostat (VMP3, Biologic) and a 10 A current booster (Biologic). Chronopotentiometric holds of 21.5 min were applied at 25, 50, 100, 200, 300, 400, and 500 mA/cm^2 where 25 mA/cm^2 was used as a conditioning step. Pulsed electrolysis (PE) was performed by cycling between the desired operating current density for 40 s and 1 mA/cm^2 for 20 s.

Anode stability tests were performed in the same setup and under the same electrochemical protocol, except the cathode was switched to an HER cathode as described above.

Product Quantification

Cathodic tail gas is directly fed into an online gas chromatograph (GC, Agilent 8890A) equipped with two Plot-Q columns, a Molseive column, a flame ionization detector, and a thermal conductivity detector. During PE the GC injection was timed during the latter half of the "on" period, as indicated by Figure S9b. The flow rate of cathodic tail gas was measured with a displacement flow meter (μflow, BPC Instruments). Liquid products were collected from the anolyte after electrolysis and mixed with a D_2O standard containing 10 mM dimethyl sulfoxide (HPLC, Alfa Aesar) internal standard at a 9:1 ratio for a total of 500 μL. The liquid sample was measured using water suppression ^{1}H nuclear magnetic resonance spectroscopy (Bruker Avance III HD system equipped with a BBO Prodigy probe). Calibration curves were made with purchased chemicals and the same dimethyl sulfoxide internal standard.

In situ Surface Enhanced Raman Spectroscopy

Raman measurements were collected on a Renishaw InVia Raman microscope equipped with a water immersion objective (Leica, 63x, 0.9 NA) and 785 nm laser. The laser power was set to 300 mW, and spectra were collected with acquisition times of 10 s.

A GDE-based cell with 0.1 M $KHCO_3$ was used for *in situ* Raman spectra collection. The cell consisted of a gas chamber, a liquid chamber, and PTFE gaskets for sealing (Figure S12). A Pt wire was used as the counter electrode and a solid-state electrode (leakless Ag/AgCl, eDAQ) was used as the reference electrode. CO_2 was fed at 20 s.c.c.m. throughout the experiment. Raman spectra were collected during the "on" period of PE towards the latter half of 40s "on" time as indicated by Figure S9b.

Materials Characterizations

Powder X-ray diffraction (PXRD) was performed on zero-background single crystal Si holders using a Rigaku Ultima IV with Cu Kα radiation. A scan rate of 10° min^{-1} was used to record the PXRD patterns from the 2θ range 10–90°. Scanning electron microscopy (SEM) and elemental dispersive X-ray spectroscopy (EDX) were performed on a Hitachi SU8030 with an Oxford Aztec X-max 80 SDD EDS detector at 30 keV. X-ray photoelectron spectroscopy (XPS) was conducted on a Thermo Scientific ESCALAB 250Xi with a monochromatic Al Kα source. XPS spectra were fitted with Shirley backgrounds, using a Gaussian–Lorentzian 30/70 curve shape for Cu and a finite Lorentzian curve shape for Ir. All XPS spectra were calibrated to the C 1s peak at 284.8 eV. Contact angle measurements were performed on a goniometer (Ossila) with 10 μL of water. Inductively coupled plasma mass spectrometry (ICP-MS) was performed on a computer-controlled (QTEGRA software) Thermo iCapQ ICP-MS (Thermo Fisher Scientific, Waltham, MA, USA) operated in standard mode and equipped with an ESI SC-2DX PrepFAST autosampler (Omaha). Anolyte sample was diluted 10x with 2% HNO_3/2% HCl. Sustainion membrane was dissolved via microwave by a 30 min ramp from room temperature to 210 °C, and a 15 min hold at 210 °C.

S2. Electrode Characterizations

a) Nafion

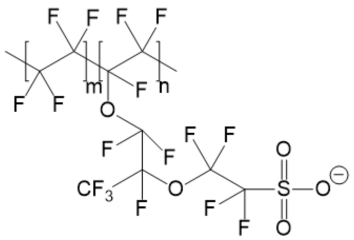

b) Sustainion XA-9

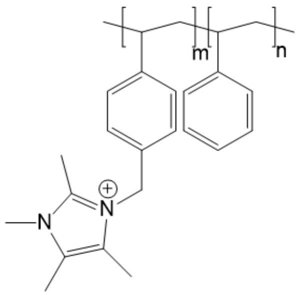

c) Fluorinated Ethylene Propylene

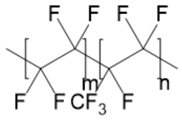

Figure S1. Chemical structures of (a) Nafion, (b) Sustainion XA-9, and (c) FEP binders.

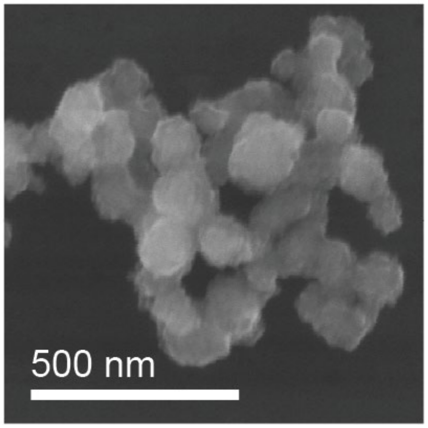

Figure S2. SEM image of commercial Cu NP as received.

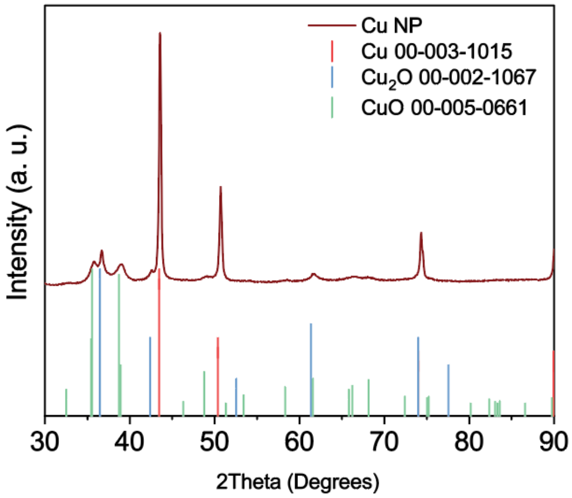

Figure S3. XRD of commercial Cu NP as received.

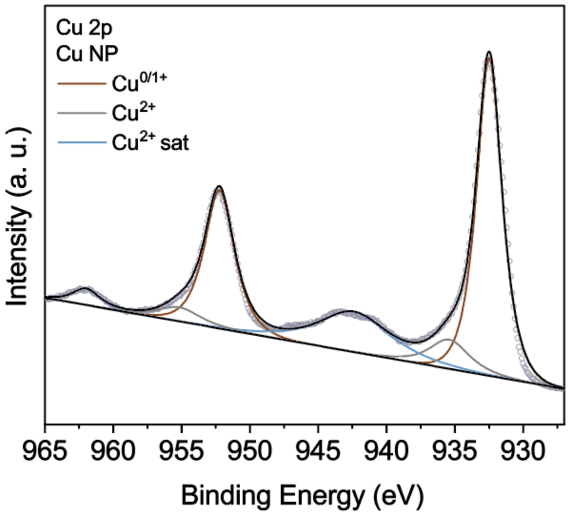

Figure S4. Cu 2p XPS of commercial Cu NP as received.

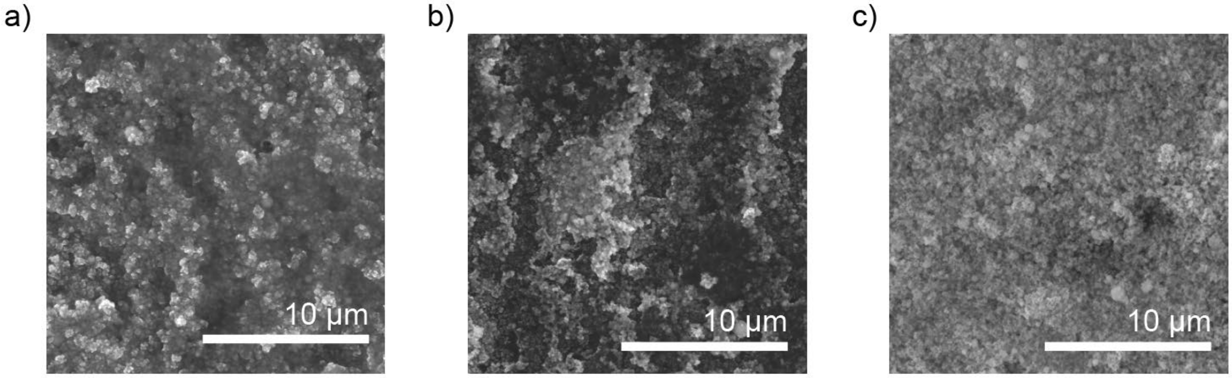

Figure S5. SEM images of spray coated Cu NP with (a) Nafion, (b) Sustainion, and (c) FEP binder on carbon paper.

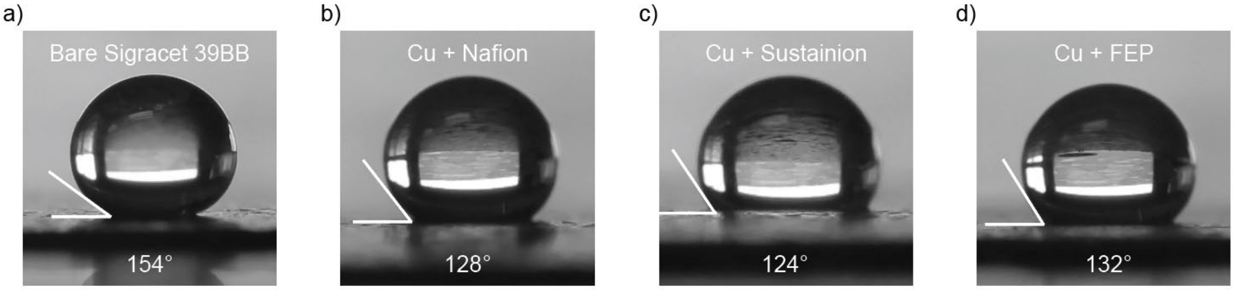

Figure S6. Water contact angle measurement of (a) bare carbon paper with microporous layer, (b) Cu NP with Nafion, (c) Cu NP with Sustainion, and (d) Cu NP with FEP.

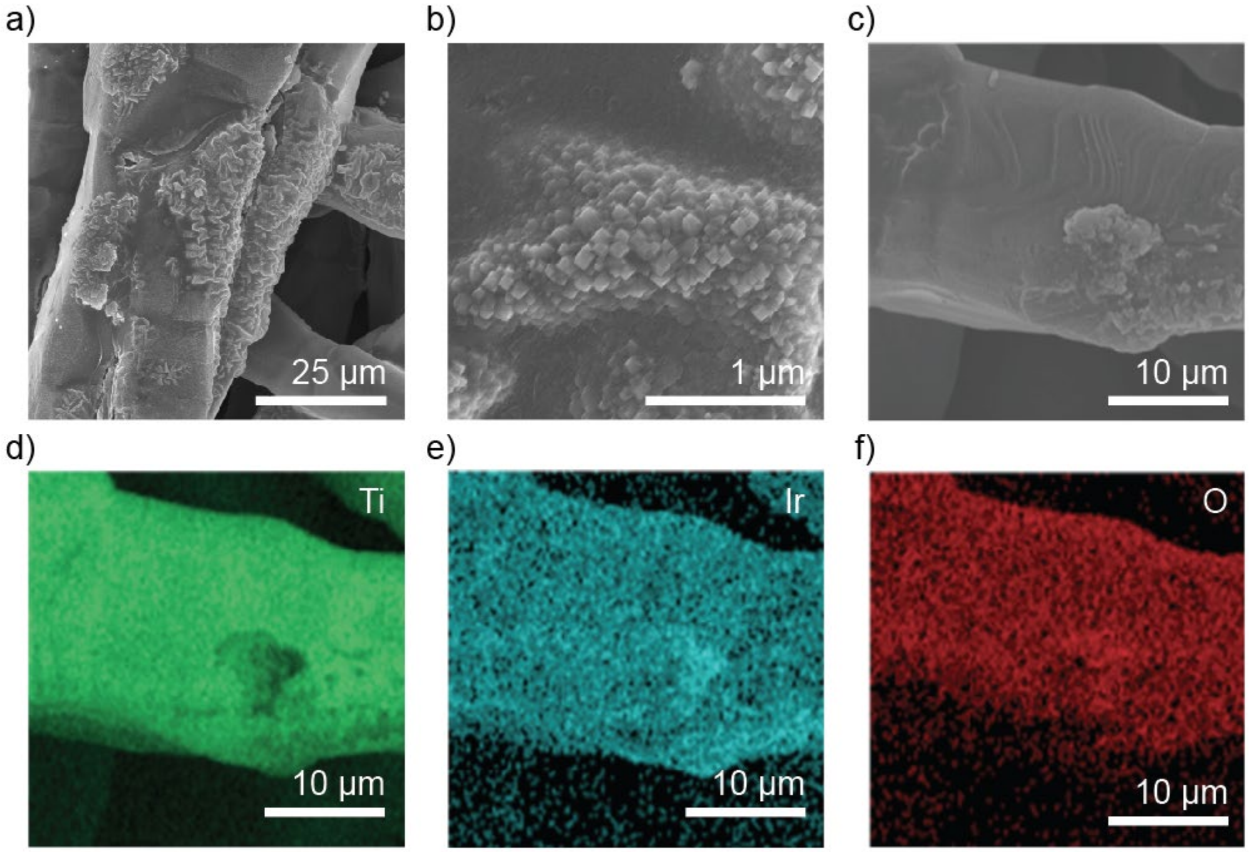

Figure S7. (a-c) SEM image of synthesized IrO_x/Ti anode. (d-f) Ti, Ir, and O EDS mappings of region shown in (c).

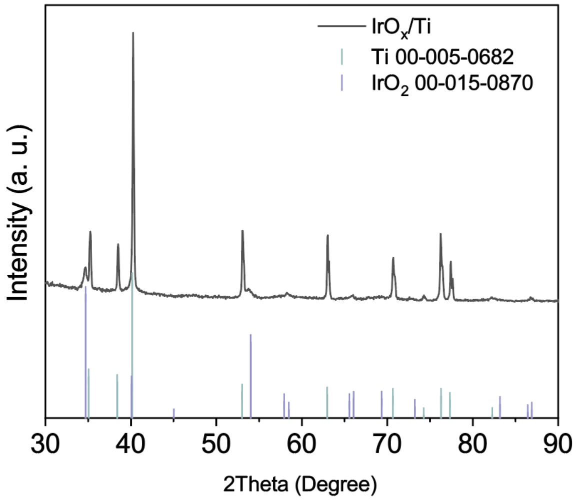

Figure S8. XRD of synthesized IrO_x/Ti anode.

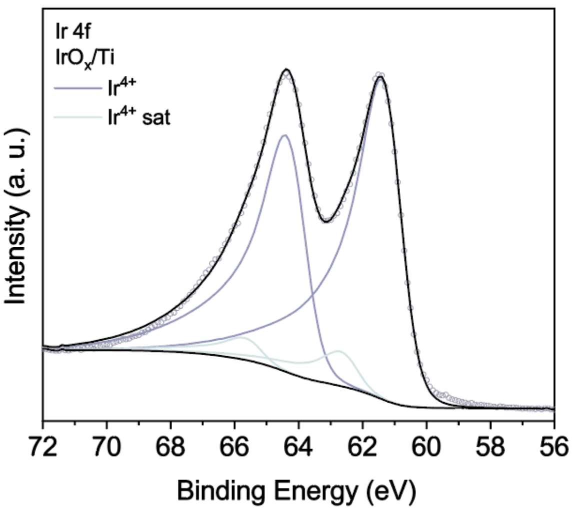

Figure S9. Ir 4f XPS of synthesized IrO$_x$/Ti anode.

S3. Electrochemical Performance

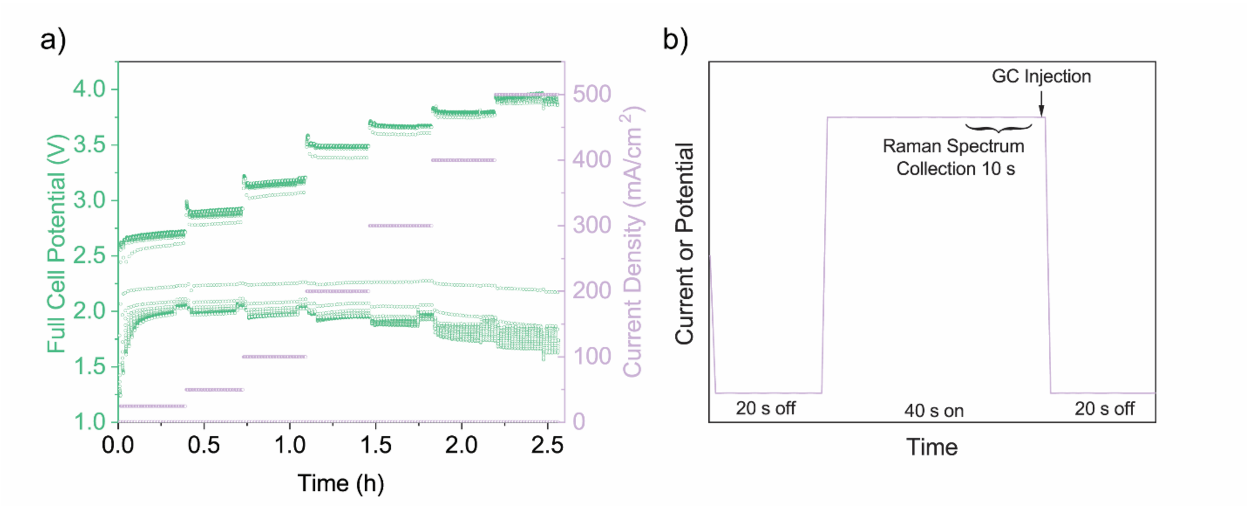

Figure S10. (a) Example of potential response from PE of full MEA cell with Cu cathode and IrO_x/Ti anode. (b) Illustration of when GC injections and Raman spectra were taken.

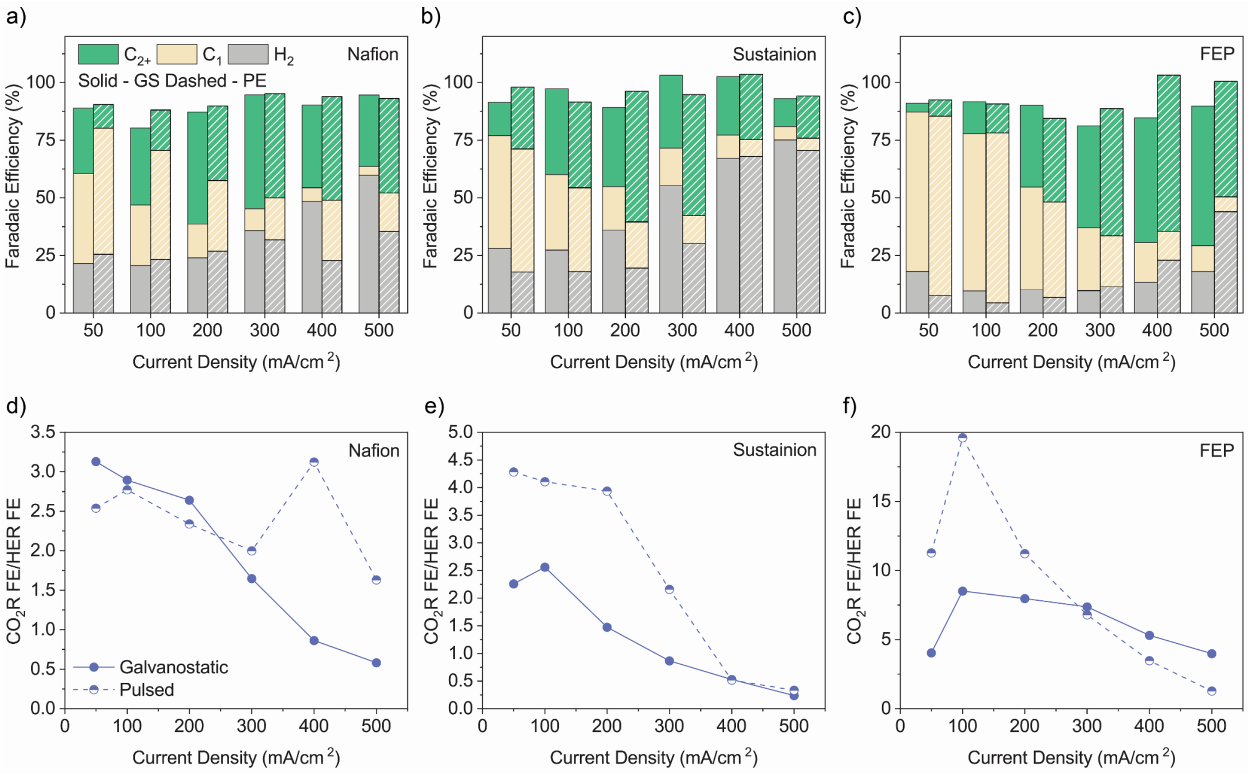

Figure S11. Faradaic efficiency of Cu NP and (a) Nafion, (b) Sustainion, and (c) FEP binders under galvanostatic (GS) and PE operations. ECR to HER ratios of Cu NP and (c) Nafion, (b) Sustainion, and (c) FEP binders under GS and PE operations

S4. *In Situ* Raman

A thicker carbon paper that is more hydrophobic was used to avoid flooding during electrolysis due to the presence of liquid electrolyte in this cell design as well. The electrolyte was chosen to be 0.1 M $KHCO_3$ to avoid local pH changes due to cation effects.[2] Prior literature has shown that PE operation enhances cation effects;[3] therefore using a dilute electrolyte may help isolate the factors of changes in local reaction environment caused by PE operation.

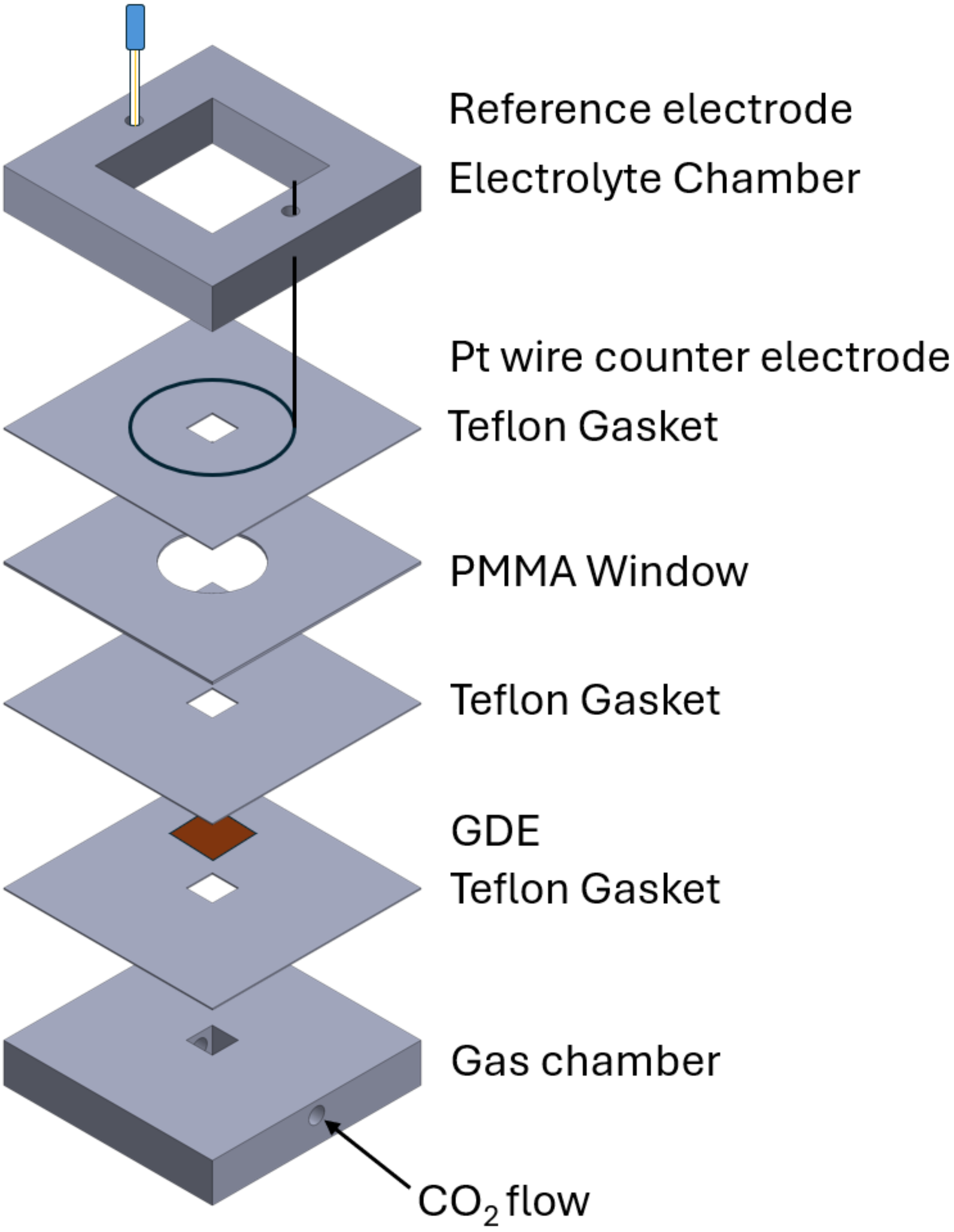

Figure S12. Schematic of *in situ* Raman cell in GDE configuration.

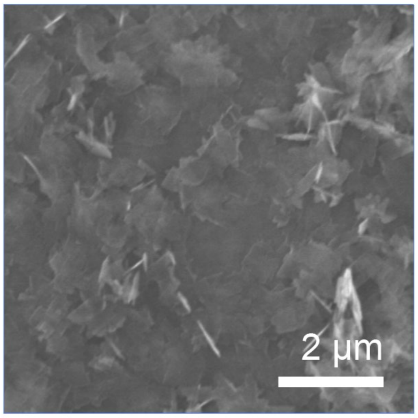

Figure S13. SEM image of synthesized CuO.

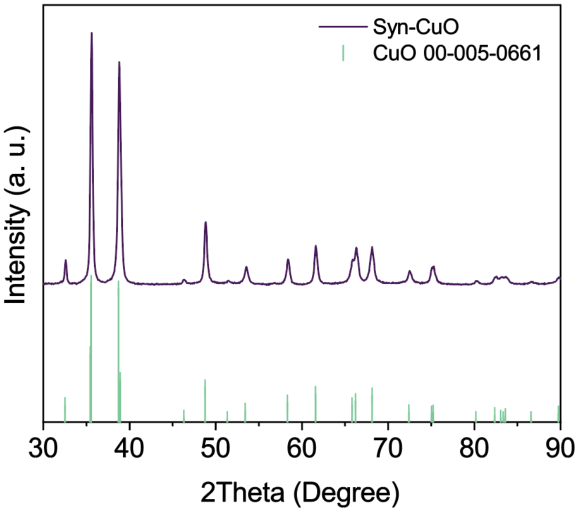

Figure S14. XRD of synthesized CuO.

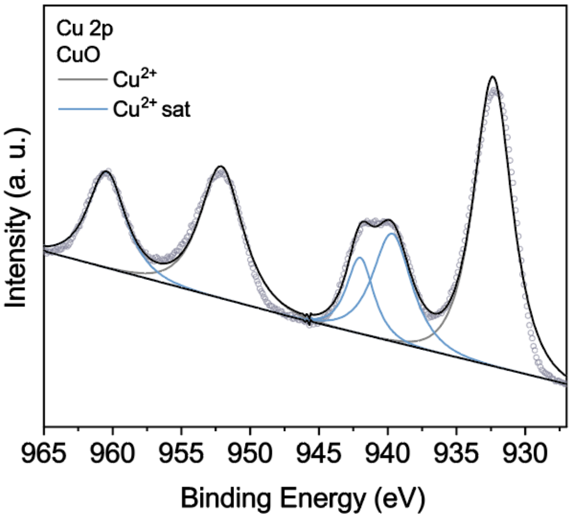

Figure S15. Cu 2p XPS of synthesized CuO.

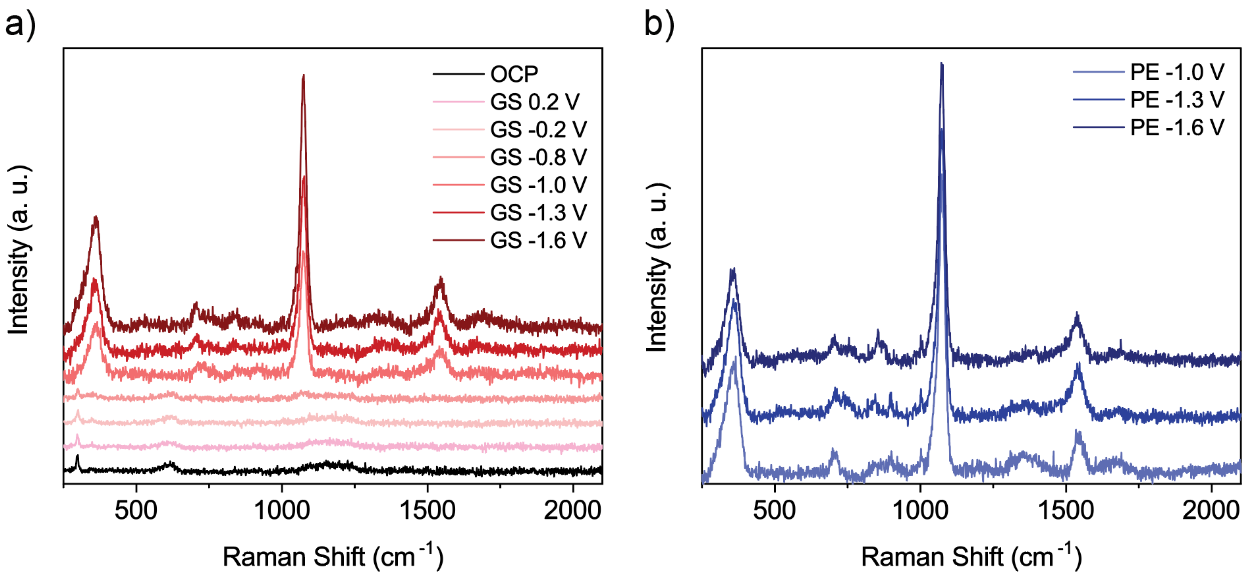

Figure S16. Raman spectra in GDE Raman cell with 0.1 M $KHCO_3$ for (a) CuO under galvanostatic GS operation from open circuit potential (OCP) to -1.6 V vs. RHE and (b) CuO under PE operation with $\boldsymbol{E_c}$ from -1.0 to -1.6 V vs. RHE and a consistent $\boldsymbol{E_a}$ = 0 V vs. RHE.

Table 1. List of peak assignments for Raman spectroscopy.

Raman Shift (cm^{-1})	Assignment	Reference
297 , 347, 610	CuO	Ref[4, 5]
362	Cu-$*CO_2^-$	Ref[6, 7]
707	Cu-*OH	Ref[8, 9]
1075	$*CO_3^{2-}$	Ref[7, 10]
1543	$*CO_2^-$	Ref[7, 10]

S5. Anode Stability Test

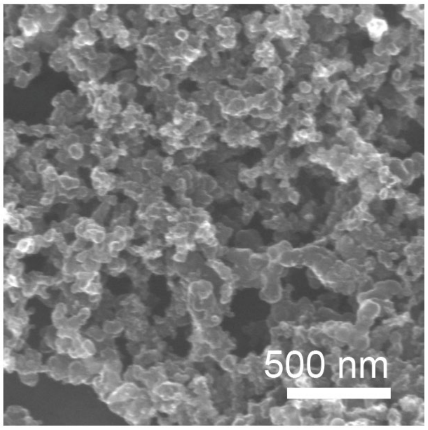

Figure S17. SEM image and EDS mapping of commercial Pt/C catalyst as received.

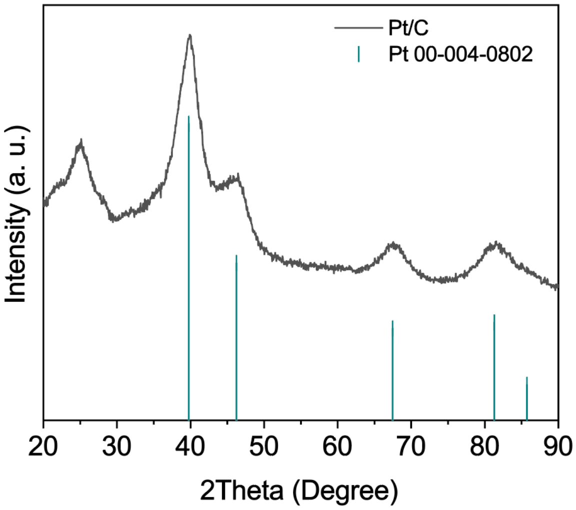

Figure S18. XRD of commercial Pt/C catalyst as received.

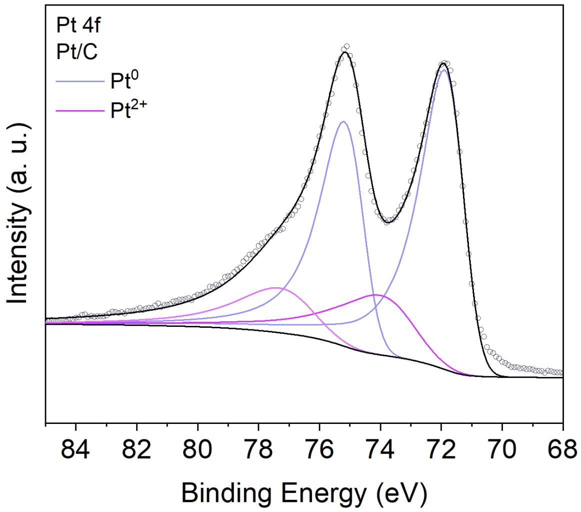

Figure S19. Pt 4f XPS spectrum of commercial Pt/C catalyst as received.

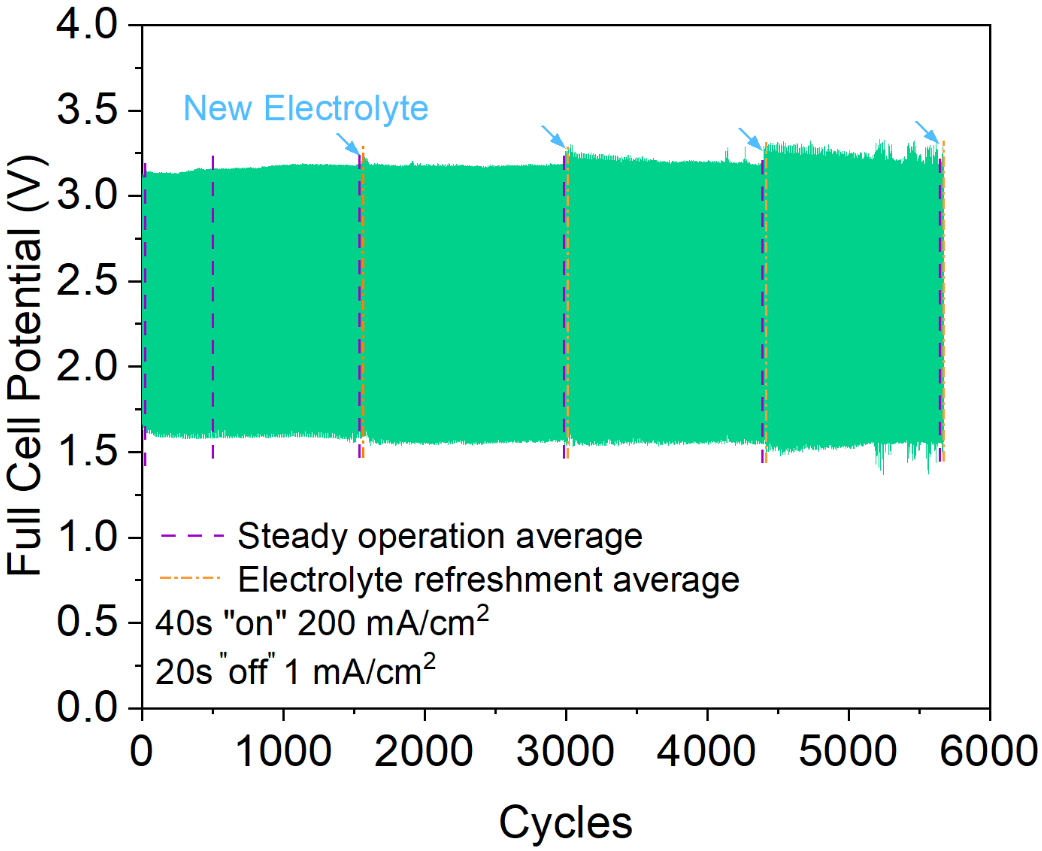

Figure S20. Labels of time intervals of when potentials of "on" periods were averaged.

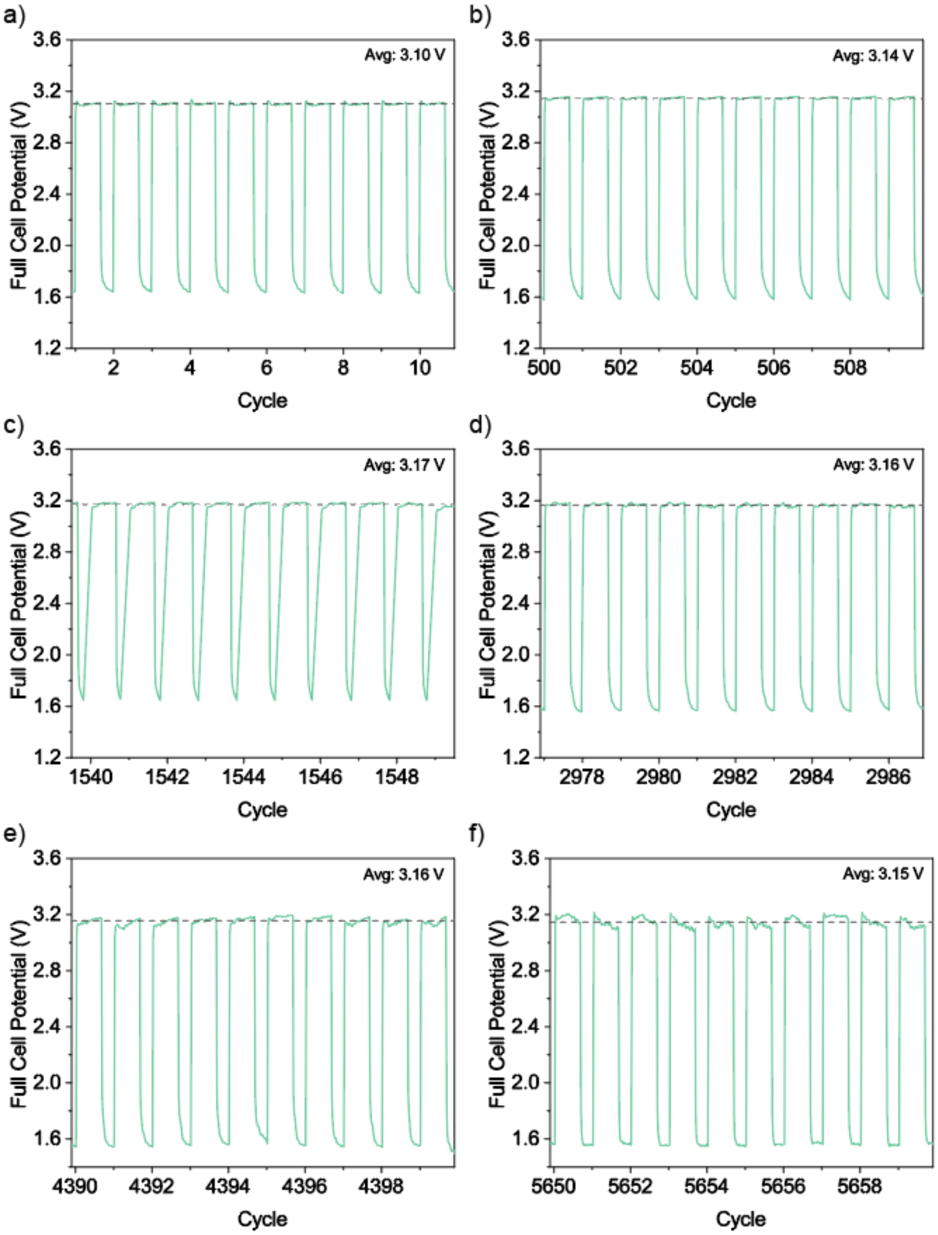

Figure S21. (a-f) Samples of potential response from stabilized PE operation at various times / cycle numbers for operation between j_c = 200 mA/cm^2 and j_a = 1 mA/cm^2 for a zero-gap MEA with a Pt/C cathode and an IrO_x/Ti anode in 0.1 M $KHCO_3$ anolyte.

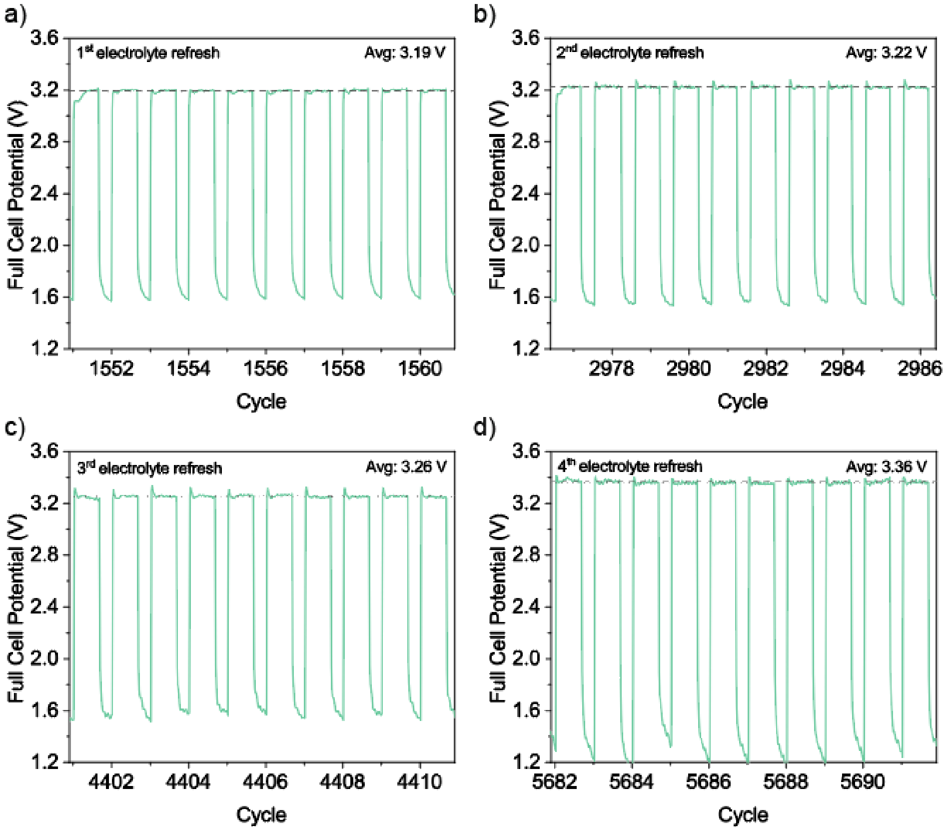

Figure S22. (a-d) Samples of potential response from PE operation immediately after each electrolyte replacement for operation between $\boldsymbol{j_c}$ = 200 mA/cm^2 and $\boldsymbol{j_a}$ = 1 mA/cm^2 for a zero-gap MEA with a Pt/C cathode and an IrO_x/Ti anode in 0.1 M $KHCO_3$ anolyte.

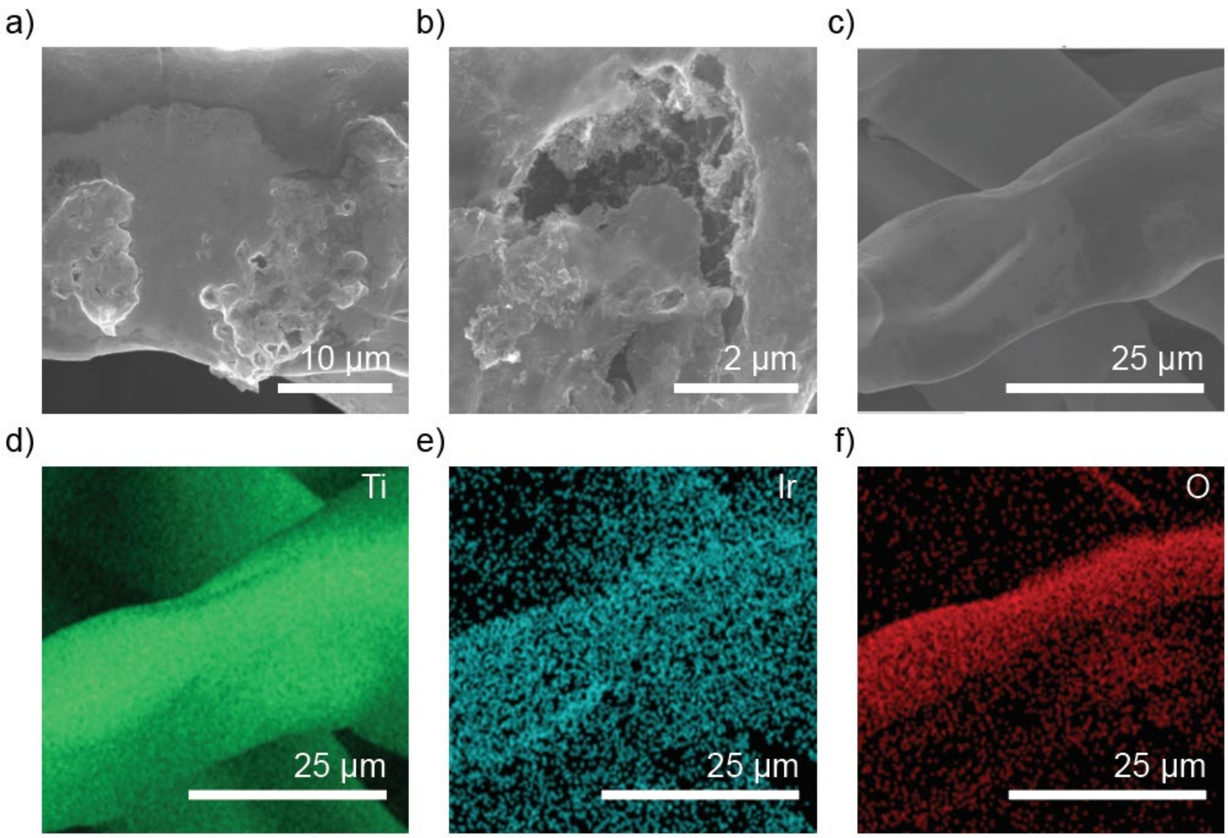

Figure S23. (a-c) SEM images of the IrO_x/Ti anode after ~5700 cycles of PE operation between $\boldsymbol{j_c}$ = 200 mA/cm^2 and $\boldsymbol{j_a}$ = 1 mA/cm^2. (d-f) Ti, Ir, and O EDS mappings of region shown in Figure (c).

The cubic IrO_x particles as shown in Figure S7 are no longer present after the long-term stability test (Figure S233). Within the smooth layer of IrO_x coating on Ti, nanoparticles of sub 100 nm were observed. The EDS mappings still show overlapping regions of Ti, Ir, and O after the stability test.

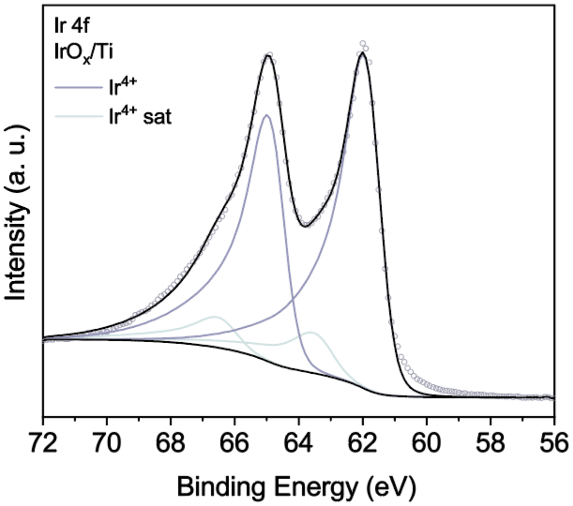

Figure S24. Ir 4f XPS spectrum of IrO$_x$/Ti after the stability test.

Acknowledgements

This work was supported by the NSF Engineering Research Center (ERC), Center for Innovative and Strategic Transformation of Light Alkane Resources (CISTAR; NSF award number EEC-1647722) and a National Science Foundation CAREER Award (2144365-CBET). This work made use of the Keck-II facility of Northwestern University's NUANCE Center, which has received support from the SHyNE Resource (NSF ECCS-2025633), the IIN, and Northwestern's MRSEC program (NSF DMR-2308691). This work made use of the EPIC facility of Northwestern University's NUANCE Center, which has received support from the SHyNE Resource (NSF ECCS-2025633), the IIN, and Northwestern's MRSEC program (NSF DMR-2308691). This work made use of the IMSERC (RRID:SCR_017874) NMR facility at Northwestern University, which has received support from the Soft and Hybrid Nanotechnology Experimental (SHyNE) Resource (NSF ECCS-2025633), Int. Institute of Nanotechnology, and Northwestern University. This work made use of the Jerome B. Cohen X-Ray Diffraction Facility supported by the MRSEC program of the National Science Foundation (DMR-2308691) at the Materials Research Center of Northwestern University and the Soft and Hybrid Nanotechnology Experimental (SHyNE) Resource (NSF ECCS-1542205.). Xiao Kun Lu would also like to thank Northwestern University's REACT core research scientist Dr. Selim Alayoglu and Aditya Menon of Seitz Lab and Sargent Group for their generous help with Raman spectroscopy.

References

1. Wang, X.; Klingan, K.; Klingenhof, M.; Moller, T.; Ferreira de Araujo, J.; Martens, I.; Bagger, A.; Jiang, S.; Rossmeisl, J.; Dau, H.; Strasser, P., Morphology and mechanism of highly selective Cu(II) oxide nanosheet catalysts for carbon dioxide electroreduction. *Nat Commun* **2021,** *12* (1), 794.
2. Hicks, M. H.; Nie, W.; Boehme, A. E.; Atwater, H. A.; Agapie, T.; Peters, J. C., Electrochemical CO2 Reduction in Acidic Electrolytes: Spectroscopic Evidence for Local pH Gradients. *Journal of the American Chemical Society* **2024,** *146* (36), 25282-25289.
3. Li, Z.; Wang, L.; Sun, L.; Yang, W., Dynamic Cation Enrichment during Pulsed CO(2) Electrolysis and the Cation-Promoted Multicarbon Formation. *J Am Chem Soc* **2024,** *146* (34), 23901-23908.
4. Deng, Y.; Handoko, A. D.; Du, Y.; Xi, S.; Yeo, B. S., In Situ Raman Spectroscopy of Copper and Copper Oxide Surfaces during Electrochemical Oxygen Evolution Reaction: Identification of CuIII Oxides as Catalytically Active Species. *ACS Catalysis* **2016,** *6* (4), 2473-2481.
5. Long, C.; Liu, X.; Wan, K.; Jiang, Y.; An, P.; Yang, C.; Wu, G.; Wang, W.; Guo, J.; Li, L.; Pang, K.; Li, Q.; Cui, C.; Liu, S.; Tan, T.; Tang, Z., Regulating reconstruction of oxide-derived Cu for electrochemical CO2 reduction toward n-propanol. *Science Advances 9* (43), eadi6119.
6. Zhao, Y.; Zhang, X.-G.; Bodappa, N.; Yang, W.-M.; Liang, Q.; Radjenovica, P. M.; Wang, Y.-H.; Zhang, Y.-J.; Dong, J.-C.; Tian, Z.-Q.; Li, J.-F., Elucidating electrochemical CO2 reduction reaction processes on Cu(hkl) single-crystal surfaces by in situ Raman spectroscopy. *Energy & Environmental Science* **2022,** *15* (9), 3968-3977.
7. Chernyshova, I. V.; Somasundaran, P.; Ponnurangam, S., On the origin of the elusive first intermediate of CO2 electroreduction. *Proceedings of the National Academy of Sciences* **2018,** *115* (40), E9261-E9270.
8. He, M.; Li, C.; Zhang, H.; Chang, X.; Chen, J. G.; Goddard, W. A., 3rd; Cheng, M. J.; Xu, B.; Lu, Q., Oxygen induced promotion of electrochemical reduction of CO2 via co-electrolysis. *Nat Commun* **2020,** *11* (1), 3844.
9. Bodappa, N.; Su, M.; Zhao, Y.; Le, J.-B.; Yang, W.-M.; Radjenovic, P.; Dong, J.-C.; Cheng, J.; Tian, Z.-Q.; Li, J.-F., Early Stages of Electrochemical Oxidation of Cu(111) and Polycrystalline Cu Surfaces Revealed by in Situ Raman Spectroscopy. *Journal of the American Chemical Society* **2019,** *141* (31), 12192-12196.
10. Niu, Z.-Z.; Gao, F.-Y.; Zhang, X.-L.; Yang, P.-P.; Liu, R.; Chi, L.-P.; Wu, Z.-Z.; Qin, S.; Yu, X.; Gao, M.-R., Hierarchical Copper with Inherent Hydrophobicity Mitigates Electrode Flooding for High-Rate CO2 Electroreduction to Multicarbon Products. *Journal of the American Chemical Society* **2021,** *143* (21), 8011-8021.